

# Structural, Kinetic and Cytotoxicity Aspects of 12–28 $\beta$ -Amyloid Protein Fragment: A Reappraisal

FRANCESC RABANAL,<sup>a</sup> JOSEP M. TUSELL,<sup>c</sup> LLUIS SASTRE,<sup>a</sup> M. ROSA QUINTERO,<sup>a</sup> MONTSE CRUZ,<sup>a,b</sup>  
DOLORS GRILLO,<sup>a,b</sup> MIQUEL PONS,<sup>a,b</sup> FERNANDO ALBERICIO,<sup>a,b</sup> JOAN SERRATOSA<sup>c</sup> and ERNEST GIRALT<sup>a,b\*</sup>

<sup>a</sup> Departament de Química Orgànica, Universitat de Barcelona, Martí i Franquès, 1-11, 08028 Barcelona, Spain

<sup>b</sup> Institut de Recerca Biomèdica de Barcelona, IRBB-PCB, Josep Samitier 1, 08028 Barcelona, Spain

<sup>c</sup> Departament de Neuroquímica, i Farmacologia i Toxicologia, Institut d'Investigacions Biomediques de Barcelona, CSIC-IDIBAPS, 08036 Barcelona, Spain

**Abstract:** A chemical, structural and biological study on the  $\beta$ -amyloid peptide  $\beta_{12-28}$  is reported which was carried out in order to assess the feasibility using this peptide fragment as a model of the natural  $\beta$ -amyloid protein. The aggregation properties of  $\beta_{12-28}$  have been investigated by pulse field-gradient NMR spectroscopy, Fourier transform infrared spectroscopy and transmission electron microscopy. The results obtained suggest that  $\beta_{12-28}$  behaviour is comparable to that of the natural  $\beta$ -amyloid protein although kinetically slower. Translational diffusion coefficients obtained by NMR on an aged  $\beta_{12-28}$  solution suggest that the soluble peptide fraction is composed of oligomeric intermediates adopting an extended ellipsoidal assembly rather than a spherical one. The  $\beta_{12-28}$  peptide proved to be cytotoxic in PC12 cell cultures as monitored by the MTT assay, although a lack of reproducibility was observed in the dose-response experiments. Copyright © 2002 European Peptide Society and John Wiley & Sons, Ltd.

**Keywords:**  $\beta_{12-28}$  amyloid peptide; pulse field-gradient NMR; solid phase peptide synthesis; cytotoxicity

## INTRODUCTION

Alzheimer's disease is the most common form of senile dementia. This syndrome is becoming of

Abbreviations: As in *J. Peptide Sci* **5** 465–471 (1999) and AD, Alzheimer's disease; AM resin, 4-(2',4'-dimethoxyphenyl)-Fmoc-aminomethyl)-phenoxy resin;  $\beta$ A,  $\beta$ -amyloid protein; MTT, 3-(4,5-dimethylthiazol-2-yl)-2,5-diphenyltetrazolium bromide; NMR, nuclear magnetic resonance; PC 12, rat pheochromocytoma cell line cultures; PBS, phosphate buffer saline.

\*Correspondence to: Dr Ernest Giralt, Institut de Recerca Biomèdica de Barcelona, IRBB-PCB, Josep Samitier 1, 08028 Barcelona, Spain.

Contract/grant sponsor: La Caixa de Pensions; Contract/grant number: 99/036-00.

Contract/grant sponsor: FEDER; Contract/grant number: 2FD97.0267.

Contract/grant sponsor: CICYT; Contract/grant number: SAF 2001-0067.

Contract/grant sponsor: Fundació la Marató de TV3; Contract/grant number: 010/97.

paramount importance due to the increase of life expectancy in developed countries. The hallmark of Alzheimer's disease is the extracellular deposition of amyloid plaques in the brain. A great deal of evidence, coming from genetic and neuropathologic studies, suggests that accumulation of neuritic plaques is central to the pathogenesis of the disorder [1]. The major component of senile plaque cores is a 42 amino acid protein called  $\beta$ -amyloid protein ( $\beta_{1-42}$ , see Figure 1). Other variants are also present, such as  $\beta_{1-40}$  which is present in cerebrovascular plaques together with  $\beta_{1-42}$ ,  $\beta_{1-39}$ , and truncated versions  $\beta_{x-42}$  ( $x = 2-11$ )

Despite incomplete understanding of the mechanism of the disease, several general therapeutical strategies have been suggested to essentially regulate or reduce  $\beta$ -amyloid protein production, aggregation and cytotoxic effects [2]. In this context, the search for compounds that could prevent  $\beta$ A fibrillar

Asp<sup>1</sup>-Ala-Glu-Phe-Arg-His-Asp-Ser-Gly-Tyr-Glu-Val<sup>12</sup>-His-His-Gln-Lys-Leu-Val-Phe-  
 Phe-Ala-Glu-Asp-Val-Gly-Ser-Asn-Lys<sup>28</sup>-Gly-Ala-Ile-Ile-Gly-Leu-Met-Val-Gly-Gly-Val-  
 Val-Ile-Ala<sup>42</sup>

Figure 1 Sequence of  $\beta_{1-42}$  amyloid protein. The sequence of the model  $\beta_{12-28}$  peptide is highlighted.

aggregation is a subject of intense research in order to delay or control the evolution of Alzheimer's disease. This approach requires access to considerable amounts of the protein. Although commercially available,  $\beta$ A protein is expensive and different commercial sources have been reported to yield different toxicity and aggregation properties [3]. Synthesis is also difficult and usually provides small amounts of protein due to low synthetic and chromatographic overall yields. Thus, the search for peptide models that were easy to prepare and handle, and could reproduce the fibrillogenic aggregation process of natural  $\beta$ A is of great interest in order to speed up the development of inhibitory drug candidates and to reduce the costs of the research.

Several synthetic peptide fragments have been described in the literature as models of  $\beta$ -amyloid protein [4]. Most of them include the central hydrophobic part of the protein (residues 17–21) which has been proposed to be important in the fibrillogenic properties of the protein [5]. Within this context, the peptide sequence corresponding to amino acid residues 12–28 ( $\beta_{12-28}$ ) has gathered considerable interest in the past years. The peptide  $\beta_{12-28}$  forms fibrillar structures similar to those found for the natural protein [6,7]. Recently, a detailed NMR study has shown that  $\beta_{12-28}$  solution behaviour is reminiscent of the early stages of the fibrillogenesis process [8,9]. Furthermore, it also shows a remarkable biological activity. It has been suggested that  $\beta_{12-28}$  may exert dysregulatory cognitive effects by means of a defective coordination of potassium channel function in nerve, glia and endothelial cells [10].

In this article, a detailed study of  $\beta_{12-28}$  aggregation and cytotoxic properties is presented. The advantages and limitations of using this peptide fragment as a model of the  $\beta$ -amyloid protein is finally discussed.

## MATERIALS AND METHODS

### Peptide Synthesis

Fmoc-protected amino acids were purchased from Novabiochem (Läufelfingen, Switzerland) and Perseptive Biosystems (Framingham, Massachusetts).

TBTU, Fmoc-AM handle and resin MBHA were also obtained from Novabiochem whereas HOAt and PEG-PS resin were from Perseptive Biosystems. Chemical reagents DIPCI, HOBt, triethylsilane and DMAP were from Fluka (Buchs, Switzerland). Manual and continuous flow peptide syntheses (Milligen 9050 PepSynthesizer) were performed following standard procedures unless otherwise stated. Amino-functionalized resins were derivatized with AM linker (Novabiochem) and contained Ile as the reference amino acid. Manual synthesis consisted of the following steps: (i) resin washing with DMF (5  $\times$  30 s); (ii) Fmoc removal with 20% piperidine/DMF (1  $\times$  1 min + 2  $\times$  7 min); (iii) washing with DMF (5  $\times$  30 s); (iv) acylation with Fmoc-protected amino acid (4 times of excess of Fmoc amino acid and activating reagent in minimum amount of DMF); (v) washing with DMF (5  $\times$  30 s) and CH<sub>2</sub>Cl<sub>2</sub> (5  $\times$  30 s); (vi) Kaiser's test (with a peptide-resin sample); (vii) DMF washing (5  $\times$  30 s). Acylations in the continuous-flow syntheses were similarly carried out using a 4 times excess of reagents and the reaction time was set to 45–60 min. Cleavage of peptides was carried out by acidolysis with TFA using triethylsilane and water as scavengers (94 : 3 : 3, v/v/v) for 60–90 min. TFA was removed with N<sub>2</sub> stream and the oily residue precipitated with dry ether. Peptide crudes were recovered by centrifugation and decantation of the ether phase. The solid was redissolved in 10% AcOH and lyophilized. The homogeneity of crudes was assessed by analytical HPLC employing Nucleosil C18 reverse phase columns (4  $\times$  250 mm, 5  $\mu$ m of particle diameter and 120 Å pore size). Elution was carried out at 1 ml min<sup>-1</sup> flow with mixtures of H<sub>2</sub>O-0.045% TFA and MeCN-0.036% TFA and UV detection at 220 nm. Peptides were purified by preparative LC in a medium pressure system using glass columns (250  $\times$  25 mm) packed with Vydac-C18 (15–20  $\mu$ m particle size) and eluting with H<sub>2</sub>O-MeCN-0.05% TFA mixtures at a flow of 120 and 180 ml/h and UV detection at 220 nm. Capillary electrophoresis was performed in an Applied Biosystems 270 instrument using a citrate solution pH = 2.53, 5–20 Kv voltage and detection also at 220 nm. Peptides were finally characterized by amino acid analysis with a Beckman

6300 analyser and by MALDI-TOF or electrospray mass spectrometry with a Bruker model Biflex III or a FisonsVG-Quattro instruments, respectively. Characterization of  $\beta_{12-28}$  was carried out by amino acid analysis (Asx 2.1 (2), Ser 0.8 (1), Glx 2.3 (2), Gly 1.1 (1), Ala 1.0 (1), Val 2.8 (3), Leu 1.0 (1), Phe 2.0 (2), His 1.8 (2), Lys 2.0 (2)) and mass spectrometry ( $C_{89}H_{136}N_{26}O_{24}$ , theoretical = 1953.02 g/mol; found: MALDI-TOF 1954.40 (M + 1); ES = 1954.19 (M + 1)).

### Sample Preparation Protocol for Aggregation Experiments

Amyloid  $\beta_{12-28}$  peptide samples freshly purified and lyophilized from H<sub>2</sub>O-0.05% TFA and MeCN-0.05% TFA mixtures were dissolved in filtered (0.45  $\mu$ m pore size) PBS buffer solutions (10 mM sodium phosphate, 100 mM NaCl, pH = 7.4) at an approximate concentration of 0.4 mM (calculated by amino acid analysis) using Eppendorf vials (dust was eliminated with an argon stream). The solution was maintained at 37 °C until a precipitate was observed (10–30 days). For the NMR experiments,  $\beta_{12-28}$  was dissolved in aqueous (10% D<sub>2</sub>O in H<sub>2</sub>O) PBS at a concentration of 0.9 mM (calculated by amino acid analysis).

### NMR Diffusion Experiments

Diffusion coefficients were obtained from <sup>1</sup>H-NMR spectra using a stimulated echo sequence [11] in a Bruker Avance DMX-500 equipped with a tripled resonance probe with z-axis gradients. The temperature of the experiment was 298 K and was calibrated with the Bruker's batman software using a 4% methanol sample in methanol-d<sub>4</sub>.

Each experiment consists of nine echo spectra where the intensity of the magnetic field gradient increases progressively until the signal intensity of selected resonances (in this case, methyl resonances of valine and leucine, between 0.6 and 0.9 ppm) reaches a value which is 10% of the initial one. The resulting value of  $G$  applied ranged between 0.025 Tm<sup>-1</sup> and 0.425 Tm<sup>-1</sup>. The values of  $\delta$  and  $\Delta$  were optimized for water and held constant for the whole experiment ( $\delta = 0.007$  s and  $\Delta = 0.110$  s).

Apparent translational diffusion coefficients were obtained by non-linear fitting of the maximum line intensities of the methyl region ( $I$ ) at different field gradients to the Stejskal-Tanner equation:

$$I = I_0 \exp \left[ -\gamma^2 G^2 D_t \delta^2 \left( \Delta - \frac{\delta}{3} \right) \right]$$

where  $I_0$  is the signal intensity in the absence of gradients,  $D_t$  is the diffusion coefficient for unrestricted translational diffusion of a molecule in an isotropic medium,  $\gamma$  is the gyromagnetic constant (for proton,  $\gamma = 26.752 \times 10^7$  rad T<sup>-1</sup> s<sup>-1</sup>),  $G$  is the gradient of the magnetic field,  $\delta$  is the duration of the field gradient and  $\Delta$  is the diffusion delay.

For roughly spherical objects, the translational diffusion coefficient  $D_t$  is related to the molecular hydrodynamic radius  $R_h$  according to the Stokes-Einstein equation:

$$D_t = \frac{k_b T}{6\pi \eta R_h F}$$

where  $k_b$  is the Boltzman constant,  $T$  is the absolute temperature,  $\eta$  is the viscosity,  $R_h$  is the hydrodynamic radius of the molecule and  $F$  is a shape factor ( $F = 1$  for a sphere). Other equations apply for objects of cylindrical or ellipsoidal shape [12].

### Electron Microscopy

Transmission electron microscopy was performed on a Philips EM 301 microscope working at 80 Kv or a Hitachi H 600 AB model at 75 Kv. Suspensions of  $\beta_{12-28}$  peptide were deposited in Formvar coated copper grids (300–400 mesh size) for 30 to 120 s, excess solution was drained off with filter paper (Whatman number 5) and stained with uranyl acetate (2% w/v in water, 30 s).

### FT-IR

IR spectra were collected on a Nicolet 510 FT spectrophotometer at 4 cm<sup>-1</sup> resolution. Samples that solidified as a gel were obtained by centrifugation of aged solutions of peptide in phosphate buffer (10 mM, pH 7.4) using D<sub>2</sub>O. Peptide gels were applied onto BaF<sub>2</sub> cell windows and dried under a heat lamp. Spectra (10 scans averaged) were recorded directly on peptide films.

### Cell Culture Assays

PC 12 pheochromocytoma cell lines were routinely cultured in Dulbecco's modified Eagle's medium containing 10% fetal bovine serum, 5% horse serum, 1% glutamine and 1% penicillin/streptomycin. Exponentially growing cells were plated at 30 000 cells per well per 100  $\mu$ l of fresh medium in 96-well tissue cultures plates.

Toxicity assays were carried out by measurement of MTT reduction. Two days after plating cells

were treated with different concentrations of aged  $\beta_{12-28}$  peptide. After 22 h, MTT (5 mg/ml) was added and incubation was continued for a further 2 h. Cells were lysed and after 24 h at 37 °C, colorimetric determination of MTT reduction was made at 550 nm. Positive controls consisted of cells in culture medium. Assay values obtained with these controls were taken as 100% viability.

## RESULTS

### Synthesis

In spite of the high degree of optimization and development achieved in peptide synthesis, some sequences still remain troublesome. Sequences that involve subsets of hydrophobic and  $\beta$ -branched amino acids (such as transmembrane sequences) are difficult to assemble probably due to intermolecular association and aggregation of the growing resin-bound peptide [13,14]. The  $\beta$ -amyloid protein contains such a type of sequence in the C-terminal end. In addition, the sparing solubility of  $\beta$ A in both aqueous and organic solvents makes purification a laborious task and usually it results in low recovery yields.

A peptide fragment,  $\beta_{12-28}$ , was chosen to investigate structurally and biologically its suitability as a model of the natural  $\beta$ -amyloid protein. The preparation of  $\beta_{12-28}$  was not straightforward though, and required some optimization effort. Initially, the assembly of this peptide in its C-terminal amide form was performed manually following essentially a standard Fmoc/<sup>t</sup>Bu chemistry protocol with carbodiimide/HOBt activation of the carboxyl function of amino acids. An AM-MBHA-polystyrene resin with a functionalization of 0.45 mmol/g resin was used. The last three residues, His<sup>14</sup> to Val<sup>12</sup>, were recoupled with TBTU/DIEA since a slightly positive Kaiser test was obtained. HPLC purification of the crude yielded an apparently homogeneous product by analytical HPLC. Surprisingly, MALDI-TOF mass spectrometry analysis of the purified fraction showed two peaks. In addition to the expected product, a contaminant with an M-128 mass was detected. Initially, two deletion compounds were considered as potential byproducts: a peptide lacking either a lysine or a glutamine. Capillary electrophoresis allowed both peaks to be separated as shown in Figure 2. The similarity of the retention times of both peptides suggests that glutamine and not lysine was missing in the byproduct. A lysine deletion would

have implied the loss of a positive charge in the molecule leading to very different HPLC and electrophoretic mobilities.

In order to avoid the formation of the deletion peptide, an improved synthesis protocol was necessary. Initially, an automatic continuous-flow synthesis was undertaken employing a TBTU/HOBt/DIEA activation protocol (4 times excess of reagents and 60 min acylation time). The amount of M-128 mass byproduct decreased substantially but not to satisfactory levels (data not shown). In a third attempt, a mixed strategy was considered. In this case, a PEG-PS support with a lower functionalization (0.17 mmol/g resin) was used to reduce the risk of intermolecular aggregation of growing peptide chains. The first 14 residues (from Lys<sup>28</sup> to Gln<sup>15</sup>) were assembled automatically. A single coupling (45 min recirculation time) using TBTU/HOBt/DIEA (5:5:10) was applied to the C-terminal sequence Phe<sup>20</sup>-Lys<sup>28</sup>. A systematic double acylation protocol employing TBTU/HOAt/DIEA (5:5:10) was applied to the segment including Phe<sup>19</sup> to Gln<sup>15</sup>. At this point, the synthesis was continued manually. To avoid the eventual growth of peptide chains lacking a Gln<sup>15</sup> residue, exhaustive acetylation of unreacted amino groups was carried out. The remaining amino acids were assembled checking the completion of reactions with the Kaiser's test. Double couplings were necessary for the remaining three amino acids. At the end of the synthesis, the HPLC purified product was analysed by capillary electrophoresis showing that the proportion of the deletion byproduct decreased to values around 1% (Figure 2). Mass spectrometry analysis by MALDI-TOF also confirmed the obtention of the desired product and the practical absence of the M-128 signal.

### NMR Diffusion Experiments

Pulsed-field NMR spectroscopy is a well-established technique to measure diffusion coefficients of soluble, low to medium molecular weight compounds [8,15,16]. The diffusion coefficient of a compound is a solvodynamic property that depends on the molecular size and shape of the sample in addition to the environment conditions (solvent, temperature, etc). Hence, this technique could be useful to study the aggregation of amyloidogenic peptides particularly in the early stages of the process.

Series of pulsed-field gradient NMR experiments were repeated over a week's period on a sample of  $\beta_{12-28}$  peptide in aqueous buffer containing 10% D<sub>2</sub>O. The apparent translational diffusion

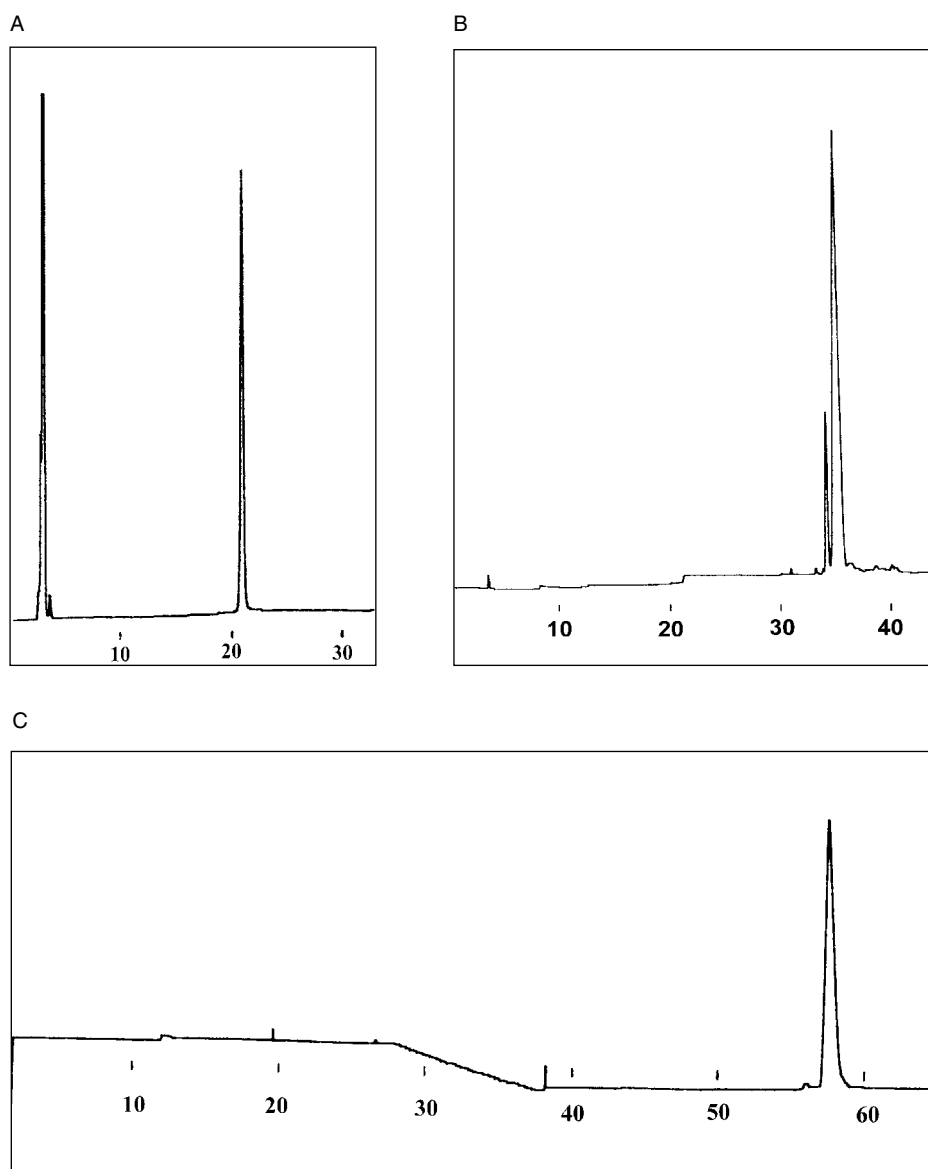


Figure 2 HPLC (register A) and CE (register B) of purified  $\beta_{12-28}$  corresponding to the first synthesis. HPLC elution conditions: 10% to 40% of B in 30 min (A = H<sub>2</sub>O-0.045% TFA; B = MeCN-0.036% TFA). CE elution conditions (B): citrate buffer, pH 2.53, injection 10 s/voltage 10 Kv. Register C corresponds to the third and successful synthesis of  $\beta_{12-28}$ . CE elution conditions (C): citrate buffer, pH 2.53, injection 1 s, voltage 5 Kv (see text for explanation).

coefficients  $D_t$  decreased as a function of time in a non-linear way as shown in Figure 3. The intensity of the spectra obtained without gradients was reduced up to ca. 50% of the initial value at the end of the 7 days experiment. The appearance of the sample at this stage was that of a highly gelatinous suspension. An amino acid analysis of the sample after centrifugation revealed that approximately half of the peptide was still not precipitated. Thus, NMR is sampling the peptide

population that is not sedimented by centrifugation, with practically no contribution from very high molecular weight species.

The translational diffusion results show that in the first hours (day 0), the soluble fraction is composed mainly of monomer species. Interestingly, the soluble fraction progresses toward higher molecular weight oligomers with time approaching a plateau value with  $D_t \sim 0.30 \times 10^{-10} \text{ m}^2 \text{ s}^{-1}$  towards the end of the experiment. For a spherical particle, this

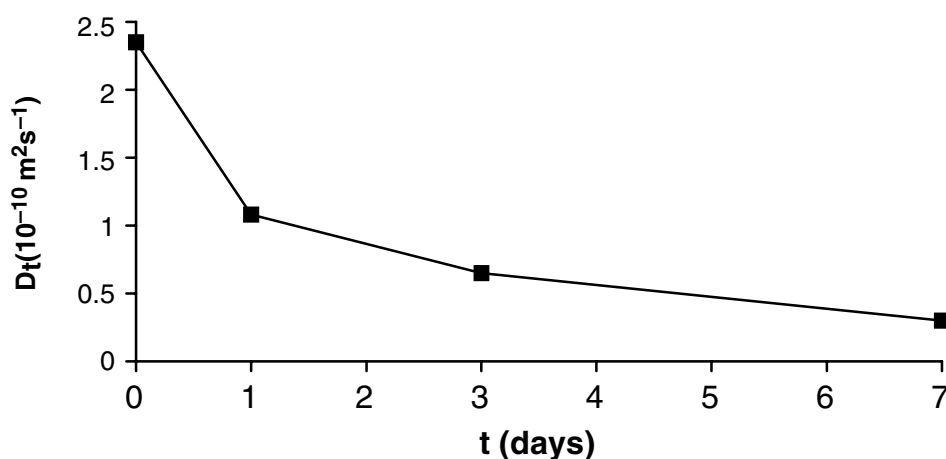


Figure 3 Diffusion coefficients of  $\beta_{12-28}$  soluble fraction over a week's period.

Table 1 Diffusion Coefficient and Molecular Hydrodynamic Radius (assuming  $F = 1$ ) of  $\beta_{12-28}$  Soluble Fraction

Time (days)	Dt ( $10^{-10} \text{ m}^2 \text{ s}^{-1}$ )	Molecular radius ( $\text{\AA}$ )
0	2.4	16
1	1.1	35
3	0.7	59
7	0.3	126

corresponds to a molecular hydrodynamic radius of 126  $\text{\AA}$ , an eight-fold increase from the initial value (see Table 1). For a uniform density particle this would imply a 500-fold increase in molecular weight that would lead to a very broad unobservable NMR signal. Assuming an aggregation geometry in which spherical particles pack linearly to form a cylinder with the same diameter of the starting particle but increasing length, diffusion coefficients of  $0.3\text{--}0.5 \times 10^{-10} \text{ m}^2 \text{ s}^{-1}$  would be expected for oligomers with 12–25 units. Similar aggregation

numbers are obtained assuming an ellipsoidal shape with the minor diameter set by the molecular dimension of the monomer. As the aggregation number increases, diffusion coefficients become very insensitive to further increases in the molecular weight.

#### FT-IR Spectroscopy

Fourier transform infrared spectroscopy can provide qualitative and semiquantitative information about the secondary structure of peptides and proteins both in solution and in the solid state. The amide carbonyl stretching band (amide I band) is sensitive to the secondary structure of the polypeptide chain [17]. In the present study, FT-IR was used to investigate the conformation of  $\beta_{12-28}$  in the fibrillar aggregates. Thus, a film of the peptide in the gel state (precipitated from a  $\text{D}_2\text{O}$  buffered solution) was analysed and the infrared spectrum obtained is displayed in Figure 5. A strong absorbance centered  $ca\ 1621 \text{ cm}^{-1}$  is observed which corresponds to the amide I band (in  $\text{H}_2\text{O}$  is shifted to slightly higher wavenumbers). This feature is characteristic of a homogeneous intermolecular  $\beta$ -sheet structure. Furthermore, the weak absorbance that appears as

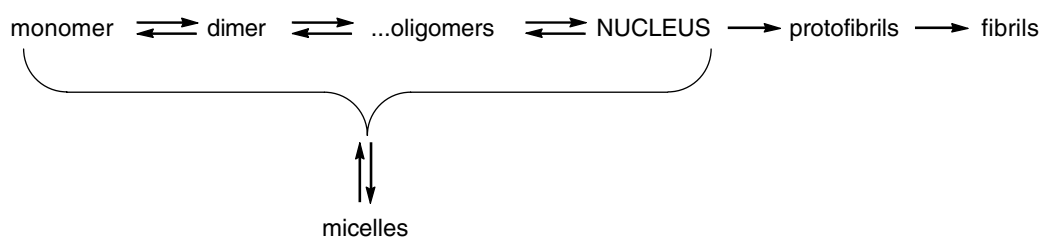


Figure 4 Nucleation-dependent mechanism of  $\beta\text{A}$  aggregation [4,30].

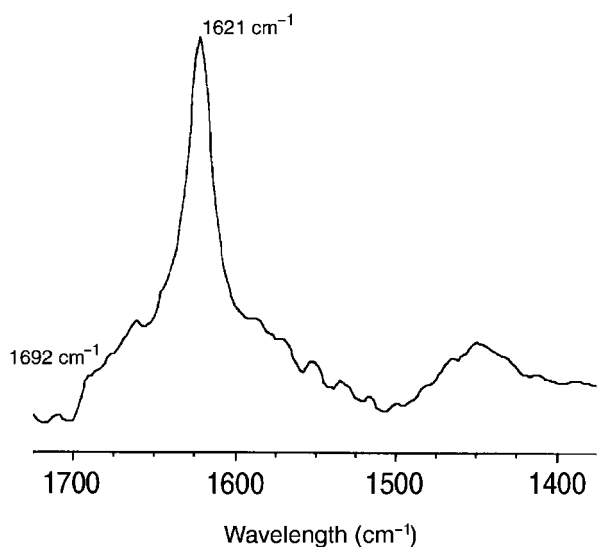


Figure 5 FT-IR spectrum of a film of  $\beta_{12-28}$  peptide in the gel state (precipitated from a  $D_2O$  buffered solution). The position of the amide I band and the weak shoulder absorbance at ca.  $1690\text{ cm}^{-1}$  are in perfect agreement with the antiparallel cross- $\beta$  pleated sheet secondary structure postulated for natural  $\beta$ -amyloid proteins.

a shoulder at ca.  $1690\text{ cm}^{-1}$  is considered to be a diagnostic for an antiparallel arrangement of the  $\beta$ -structure [18]. The broad absorption band around  $1655\text{ cm}^{-1}$  may be attributed to asparagine and/or glutamine amide side chains.

In summary, the FT-IR spectrum obtained for  $\beta_{12-28}$  is in perfect agreement with the structure generally accepted for natural  $\beta A$  when aggregated in the amyloid state, i.e. a cross- $\beta$  pleated sheet secondary with strands assembled presumably in an antiparallel fashion and oriented orthogonally to the fibril axis [4].

### Transmission Electron Microscopy Studies

The peptide  $\beta_{12-28}$  has already been shown in the literature to form fibrils in aqueous solutions. The fibrils obtained were shown to be birefringent on Congo Red binding and displayed a similar morphology to those obtained with fibrils from AD brains. In fact, this was one of the main reasons why this sequence was chosen as a putative  $\beta$ -amyloid model in the present study. The amyloidogenic properties of  $\beta_{12-28}$  could be confirmed in this work. Analysis by transmission electron microscopy of aggregated/precipitated peptide samples obtained from aqueous solutions showed the typical fibrillar structure of  $\beta$ -amyloid peptides (Figure 6).

In our hands though, fibrillar precipitates were often accompanied by variable amounts of amorphous aggregates. Similar results have also been described elsewhere [19]. Furthermore, obtention of precipitates from PBS solutions at concentrations around  $300\text{--}400\text{ }\mu\text{M}$  required unpredictable amounts of time, from 10 to 30 days approximately.

Morphology of fibrils showed some variability in the different batches prepared in spite of the control of experimental variables (pH, type of buffer, ionic strength, temperature) including those related to the sample's record (purification and lyophilization conditions of the purified sample...) [3]. In some cases, the fibrils obtained were reminiscent of those expected for amyloid aggregates. In other cases, their appearance looked like tapes or ribbons. Sometimes, they also appeared as intricate bundles of many fibrils (Figure 6). Length and thickness of fibrils were also variable. Generally speaking, all these observations correspond well with the different morphologies reported in the literature for  $\beta$ -amyloid aggregates. In fact, different studies seem to indicate that longer  $\beta$ -amyloid peptide fragments tend to yield fibrils akin to natural ones while shorter peptides produce fibrillar structures of varying diameters, thinner or thicker than typical AD fibrils. Several examples showing fibrils as thin filaments or as broad multiple-assembled ribbons are available in the literature. Altogether, heterogeneity in fibril assembly may be explained by the generally accepted mechanism of  $\beta$ -amyloid fibril organization by which peptide chains can assemble into subprotofilaments, protofilaments, filaments and finally fibrils (Figure 4) [19,20].

### Cellular Toxicity Assays

The cytotoxic effects of  $\beta_{12-28}$  peptide fragment were studied on rat pheochromocytoma cell line cultures (PC12). This line of cells is an adequate model to investigate cytotoxicity caused by  $\beta$ -amyloid since it is highly sensitive to this family of peptides and even the morphological features characteristic of apoptotic death have been observed in this biological system [21]. Cell viability was measured using the MTT assay. This test is widely used as a parameter of cell survival and proliferation. MTT, a pale yellow compound, is transformed into a blue formazan product by mitochondrial enzymes. Generally speaking, a decrease in the formation of such blue dye is understood as impairment in the enzymatic activity of mitochondria without necessarily implying cell death, although it can

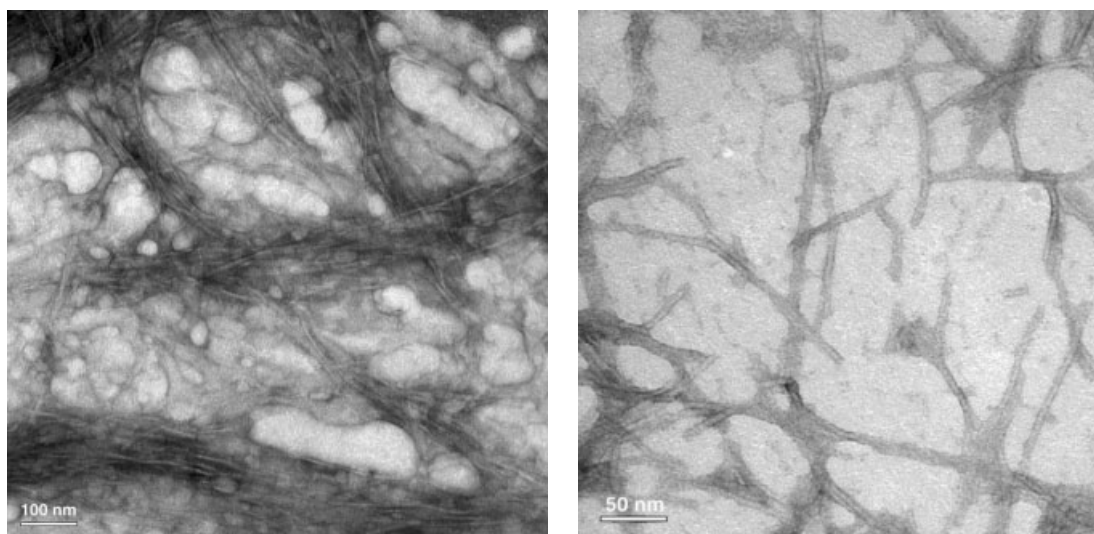


Figure 6 TEM of  $\beta_{12-28}$  aggregates. Different morphologies may be obtained such as isolated fibrils (right) or bundles of them (left).

finally progress to this point. Lately, though, it has been suggested that the  $\beta$ -amyloid peptide alters cell membrane integrity making cells vulnerable to additional toxic insults such as the formazan product generated by MTT reduction [22].

Regarding  $\beta_{12-28}$  effects on cell viability, different levels of toxicity were evidenced depending on the aggregation state of peptide. Thus, freshly prepared solutions of  $\beta_{12-28}$  were non-toxic as expected, while aged solutions produce generally significant decreases in the MTT mitochondrial reduction by PC12 cells. In Figure 7, a typical dose-response curve showing a sigmoidal decrease of cell mitochondrial activity with increasing  $\beta_{12-28}$  concentration is displayed. Unfortunately, this was not always the case in the different assays performed. The cytotoxic studies showed a similar kind of behaviour to that described above for the TEM studies. In spite of very careful control of all the experimental parameters (including the sample treatment), dose-response curves were poorly reproducible. In contrast with the curve displayed in Figure 7, other experiments resulted in non-sigmoidal dose-response dependence and/or smaller decrease in the toxicity at high concentrations.

## DISCUSSION

Synthetic peptides have proven to be valuable tools in the systematic study of the assembly and organization of  $\beta$ -amyloid fibrils as well as in the

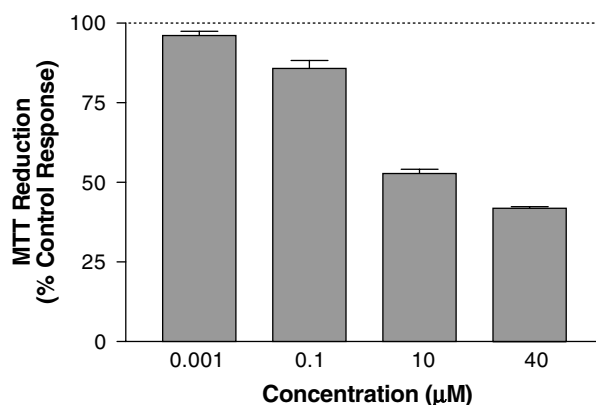


Figure 7 Cytotoxicity of aggregated (aged)  $\beta_{12-28}$  peptide in PC 12 cell cultures. A decrease in the reduction of MTT is an indicator of impairment in the enzymatic activity of mitochondria and thus of cell survival and proliferation. Data are expressed as % control values and are the arithmetic mean  $\pm$ SD of 9 replicates.

mechanistic aspects of amyloidogenic aggregation *in vitro* [4]. Many synthetic peptide fragments have been used to reproduce the behaviour of the natural protein, although the cytotoxicity of many of them remains unknown.

Generally speaking,  $\beta$ -amyloid truncation or amino acid substitution alters the process of peptide assembly and kinetics. Nevertheless, peptides as short as nine residues are able to form fibrils, such as  $\beta_{34-42}$  [23]. Peptide fragments corresponding to the N-terminal, C-terminal or the central region of



the protein have also been shown to produce amyloid aggregates. Some of the most studied include  $\beta_{1-28}$ ,  $\beta_{34-42}$ ,  $\beta_{12-28}$  and  $\beta_{10-35}$ . Morphology has also been observed to depend on the length of the peptide, with longer sequences yielding fibrils more similar to those obtained with natural varieties. One particularly interesting peptide derived from the  $\beta$ -amyloid protein is the fragment  $\beta_{25-35}$ . Like many of the other peptide models,  $\beta_{25-35}$  is not found naturally in the AD brain yet it has been widely demonstrated that it produces toxic effects similar to the natural sequence  $\beta_{1-42}$ , even when freshly prepared. Surprisingly, the C-terminal amidated version is non-toxic. These facts led recently to the proposal of a different hypothesis to explain the toxicity of  $\beta_{25-35}$ , based on a radical oxidative mechanism involving the C-terminal methionine rather than on the biological effects caused by an ordered array of assembled peptide chains. However, the role of Met<sup>35</sup> in this hypothetical radical mechanism is controversial [24]. Altogether, these precedents prompted us to choose a non-methionine containing peptide sequence, such as  $\beta_{12-28}$ , as a model of  $\beta$ -amyloid protein. The results obtained confirmed that  $\beta_{12-28}$  shows aggregation properties akin to its natural counterpart, yielding fibrillar structures as evidenced by TEM (Figure 6). Furthermore, FT-IR proves that  $\beta_{12-28}$  fibrillar aggregates adopt an antiparallel  $\beta$ -structure.

A pulse field-gradient NMR kinetic experiment showed that the soluble fraction is mainly composed of monomeric  $\beta_{12-28}$  in the beginning of the experiment as judged by the value of the diffusion coefficient ( $D_t = 2.35 \times 10^{-10} \text{ m}^2 \text{ s}^{-1}$ ; molecular hydrodynamic radius = 16 Å). This is in perfect agreement with data recently reported in the literature for  $\beta_{1-40}$  [8,15]. A diffusion coefficient of  $1.5 \times 10^{-10} \text{ m}^2 \text{ s}^{-1}$  has been found for this protein which corresponds with the monomer/dimer aggregation states [25]. The aggregation state of  $\beta_{12-28}$ , though, progresses toward higher molecular weight species with time (Figure 3). At the end of the 7 day experiment, the diffusion coefficient reaches a plateau with a value of  $0.3 \times 10^{-10} \text{ m}^2 \text{ s}^{-1}$ . This small value is not compatible with a globular type of aggregate as its hydrodynamic radius (126 Å) would imply a molecular weight unobservable by NMR. In this case, an ellipsoidal type of aggregate would adjust better to this experimental result. More precisely, an extended array of 12–25 packed  $\beta_{12-28}$  peptide chains would be compatible with such a diffusion coefficient. In the literature, oligomeric intermediates have also been suggested for  $\beta_{1-40}$

and  $\beta_{1-39}$  aggregation processes, such as ring-like structures consisting of pentamers/hexamers or octamers, according to quasielastic and static light scattering studies. These ring-like structures were proposed to act as aggregation nuclei and later polymerize by incorporation of additional  $\beta$ -sheet dimers to finally produce fibrils [26,27].

In spite of the fact that only the early stages of fibrillogenesis are observed by pulse field-gradient NMR, the study of changes in the time evolution or population of associated  $\beta$ A molecules could be of great help to study the efficacy and role of fibrillogenesis inhibitors. In fact, it has recently been suggested that oligomeric states are the intermediates responsible for neurotoxicity (synaptotoxicity) rather than the high molecular aggregates and fibrillar structures [28,29].

As far as its biological activity is concerned, we observed that  $\beta_{12-28}$  is indeed cytotoxic to PC12 cell cultures as monitored by the impairment of the mitochondrial function. Inhibition of MTT reduction may be a primary causal event in a cascade of degenerative signalling mechanisms that ultimately results in cell death. In spite of this qualitative result, a lack of reproducibility in the dose-response dependence and potency of  $\beta_{12-28}$  cytotoxicity was evidenced in this study. We believe this erratic behaviour could be related to the variable amounts of fibrillar vs amorphous aggregates obtained in the different experiments carried out. This fact, unfortunately, prevents the systematic use of  $\beta_{12-28}$  in the screening and evaluation of potential inhibitors of  $\beta$ -amyloid fibrillar aggregation and cytotoxicity.

In summary, the  $\beta_{12-28}$  peptide fragment has been shown to be a synthetically convenient model of the natural  $\beta$ -amyloid protein for the biophysical studies of the fibrillar aggregation process. In addition, aged  $\beta_{12-28}$  is toxic to PC12 cell cultures. However, the poor reproducibility of the toxicity profile hampers its systematic use for the quantitative assessment of the inhibitory effects of potential  $\beta$ A fibrillar aggregation inhibitors. This complex biological behaviour may be attributed to the variable amounts of fibrillar vs amorphous aggregates as well as to the variety of morphologies obtained in the different preparations.

## Acknowledgements

This investigation was supported by grants from La Caixa de Pensions (99/036-00), FEDER (2FD97.

0267), SAF 2001-0067 (CICYT, Comisión de Investigación Científica y Técnica) and from the Fundació la Marató de TV3 (010/97).

## REFERENCES

- Selkoe DJ. Translating cell biology into therapeutic advances in Alzheimer's disease. *Nature* 1999; **399**: A23–A31.
- Selkoe DJ. Alzheimer's disease: genotypes, phenotype, and treatments. *Science* 1997; **275**: 630–631.
- Zagorski MG, Yang J, Shao H, Ma K, Zeng H, Hong A. Methodological and chemical factors affecting amyloid  $\beta$  peptide amyloidogenicity. *Meth. Enzymol.* 1999; **309**: 189–235.
- Teplow DB. Structural and kinetic features of amyloid  $\beta$ -protein fibrillogenesis. *Amyloid: Int. J. Exp. Clin. Invest* 1998; **5**: 121–142.
- Hilbich C, Kisters-Woike B, Reed R, Masters CL, Beyreuther K. Aggregation and secondary structure of synthetic amyloid  $\beta$ -A4 peptides of Alzheimer's disease. *J. Mol. Biol.* 1991; **218**: 149–163.
- Castaño EM, Ghiso J, Prelli F, Gorevic PD, Migheli A, Frangione B. *In vitro* formation of amyloid fibril from two synthetic peptides of different lengths homologous to Alzheimer's disease  $\beta$ -protein. *Biochem. Biophys. Res. Commun.* 1986; **141**: 782–790.
- Fraser PE, Nguyen JT, Surewicz WT, Kirschner DA. pH-dependent structural transitions of Alzheimer amyloid peptides. *Biophys. J.* 1991; **60**: 1190–1201.
- Jarvet J, Damberg P, Bodell K, Göran Eriksson LE, Gräslund A. Reversible random coil to  $\beta$ -sheet transition and the early stage of aggregation of the A $\beta$ (12–28) fragment from the Alzheimer peptide. *J. Am. Chem. Soc.* 2000; **122**: 4261–4268.
- Jayawickrama DA, Shana Z, Van der Velde D, Effiong RI, Larive CK. Conformational analysis of the  $\beta$ -amyloid peptide fragment  $\beta$  (12–28). *J. Biomolec. Struct. Dynamics* 1995; **13**: 229–244.
- Flood JF, Morley JE, Roberts E. An amyloid  $\beta$ -protein fragment, A $\beta$ (12–28), equipotently impairs post-training memory processing when injected into different limbic structures. *Brain Res.* 1994; **663**: 271–276.
- Tanner JE. Use of the stimulated echo in NMR diffusion studies. *J. Chem. Phys.* 1970; **52**: 2523–2526.
- Richards EG. *An introduction to the Physical Properties of Large Molecules in Solution*. Cambridge University Press: Cambridge, 1980.
- Lloyd-Williams P, Albericio F, Giralt E. *Chemical Approaches to the Synthesis of Peptides and Proteins*. CRC: Boca Raton, FL, 1997.
- Clippingdale AB, Wade JD, Barrow CJ. The amyloid- $\beta$  peptide and its role in Alzheimer's disease. *J. Pept. Sci.* 2001; **7**: 227–249.
- Mansfield SL, Jayawickrama DA, Timmons JS, Larive CK. Measurement of peptide aggregation with pulsed-field gradient nuclear magnetic resonance spectroscopy. *Biochim. Biophys. Acta* 1998; **1362**: 257–265.
- Mansfield SL, Gotch AJ, Harms GS, Johnson CK, Larive CK. Complementary analysis of peptide aggregation by NMR and time-resolved laser spectroscopy. *J. Phys. Chem. B* 1999; **103**: 2262–2269.
- Krimm S, Bandekar J. Vibrational spectroscopy and conformation of peptides, polypeptides, and proteins. *Adv. Protein Chem.* 1986; **38**: 181–364. Seshadri S, Khurana R, Fink AL. Fourier transform infrared spectroscopy in analysis of protein deposits. *Meth. Enzymol.* 1999; **309**: 559–576.
- In fact, theoretical and experimental evidence has shown that the  $\beta$ -strands is totally antiparallel if the ratio of integrated intensities of the weak and strong components approximately at wavenumbers 1696  $\text{cm}^{-1}$  and 1625  $\text{cm}^{-1}$  ranges between 0.09 and 0.19. In this case, the ratio of absorbances obtained is approximately 0.16 (between 1621  $\text{cm}^{-1}$  and 1692  $\text{cm}^{-1}$ ) thus confirming the antiparallel nature of the  $\beta$ -structure. For further details, see: Chirgadze YN, Nevskaya NA. Infrared spectra and resonance interaction of amide-I vibration of the antiparallel-chain pleated sheet. *Biopolymers* 1976; **15**: 607.
- Walsh DM, Hartley DM, Condron MM, Selkoe DJ, Teplow DB. *In vitro* studies of amyloid beta-protein fibril assembly and toxicity provide clues to the aetiology of Flemish variant (Ala692  $\rightarrow$  Gly) Alzheimer's disease. *Biochem. J.* 2001; **355**: 869–877.
- Bohrmann B, Adrian M, Dubochet J, Kuner P, Müller F, Huber W, Nordstedt C, Döbeli H. Self-assembly of beta-amyloid 42 is retarded by small molecular ligands at the stage of structural intermediates. *J. Struct. Biol.* 2000; **130**: 232–246.
- Gschwind M, Huber G. Apoptotic cell death induced by  $\beta$  amyloid<sub>1–42</sub> peptide is cell type dependent. *J. Neurochem.* 1995; **65**: 292–300.
- Hertel C, Hauser N, Schubel R, Seilheimer B, Kemp JA.  $\beta$ -amyloid-induced toxicity: enhancement of 3-(4,5-dimethylthiazol-2-yl)-2,5-diphenyltetrazolium bromide-dependent cell death. *J. Neurochem.* 1996; **67**: 272–276.
- Jarret JT, Berger EP, Lansbury PT. The carboxy terminus of the protein is critical for the seeding of amyloid formation: implications for the pathogenesis of Alzheimer's disease. *Biochemistry* 1993; **32**: 4693–4697.
- Varadarajan S, Kanski J, Aksenova M, Lauderback C, Butterfield DA. Different mechanisms of oxidative stress and neurotoxicity for Alzheimer's A $\beta$ (1–42) and A $\beta$ (25–35). *J. Am. Chem. Soc.* 2001; **123**: 5625–5631.
- Garzon-Rodriguez W, Sepulveda-Becerra M, Milton S, Glabe CG. Soluble amyloid A $\beta$ (1–40) exists as a stable dimer at low concentrations. *J. Biol. Chem.* 1997; **272**: 21 037–21 044.

26. Tomsy SJ, Murphy RM. Kinetics of aggregation of synthetic  $\beta$ -amyloid peptide. *Arch. Biochem. Biophys.* 1992; **294**: 630–638.
27. Shen CL, Murphy RM. Solvent effects on self-assembly of  $\beta$ -amyloid peptide. *Biophys J.* 1995; **69**: 640–651.
28. Walsh DM, Klyubin I, Fadeeva JV, Cullen WK, Anwyl R, Wolfe MS, Rowan MJ, Selkoe DJ. Naturally secreted oligomers of amyloid  $\beta$  protein potently inhibit hippocampal long term potentiation *in vivo*. *Nature* 2002; **416**: 535–539.
29. Bucciantini M, Giannoni E, Chiti F, Baroni F, Formigli L, Zurdo J, Taffei N, Ramponi G, Dobson CM, Stefani M. Inherent toxicity of aggregates implies a common mechanism for protein misfolding diseases. *Nature* 2002; **416**: 507–511.
30. Lomakin A, Chung DS, Benedek GB, Kirschner DA. On the nucleation and growth of amyloid  $\beta$ -protein fibrils: Detection of nuclei and quantitation of rate constants. *Proc. Nat. Acad. Sci. USA* 1996; **93**: 1125–1129.